K-Ar Problematics of Basalts from the Triassic Succession of North Dobrogea (Romania)

Antoneta SEGHEDI[1], Ariel HEIMANN[2] and Barbu LANG[2]

[1] *Geological Institute of Romania, 1 Caransebes str., 78344 Bucharest 32, Romania*
[2] *Geological Survey of Israel, 30 Malkhe Yisrael st., Jerusalem 95501, Israel*

ABSTRACT. Submarine, tholeiitic basalt flows represent the largest part of the Triassic Niculitel Formation in the Cimmerian inverted rift of North Dobrogea, Romania. The basalts belong to an extensional deformational phase, related to rifting of the Hercynian basement of North Dobrogea. The volcanic complex consists of pillow lava, scarce tuffs or pyroclastics, dolerite dykes and minor gabbroic bodies. Discontinuous interbeds of sedimentary rocks within the section include nodular, ammonite bearing limestone, coarse epiclastic breccia, limestone turbidites and pelagic, cherty limestone. According to paleontological evidence yielded by limestone interbeds, the volcanic succession was accumulated during Late Scythian to Lower Anisian. Primary magmatic constituents are plagioclase feldspar (labrador), titanaugite, magnetite; the feldspars are replaced by a low-temperature assemblage of prehnite, pumpellyite and albite, while carbonate, chlorite and titanite replace former olivine phenocrysts. K-Ar ages of three samples (two basalts and one pillow-lava) yielded ages in the range of 142–127 Ma. The data yield a good isochron with a calculated age of 132.7 Ma (Late Valanginian) and an initial value of the $^{40}Ar/^{36}Ar$ ratio of 297.7, very close to the atmospheric ratio (295.5). The radiometric ages define a substantial difference between the K-Ar ages and the stratigraphic position (or paleontological age) of the volcanic rocks. At the present level of knowledge, it seems that the most plausible interpretation is to consider that the younger Alpine deformations are responsible for resetting the K-Ar clock.

KEY WORDS: tholeiitic basalts, Triassic, rift, Dobrogea, Romania, K-Ar age.

Introduction

The pre-Triassic basement of North Dobrogea is a segment which was offset from the Hercynian belt of Europe during the transtensional movements responsible for the breakup of Pangea. Starting in Late Permian, the Hercynian basement was subjected to rifting. Tensional history is documented by the development of shear zones in the basement and by magmatism and sedimentation during the Triassic. Compressional deformation started in Late Triassic and continued throughout the Jurassic. A large stratigraphic gap corresponds to the Early Cretaceous, as no sediments of this age are preserved, except for scarce relics of Aptian weathering crust (Radan 1994).

Previous geochronological data suggest that the main deformational events affecting the pre-Triassic basement rocks took place at the Triassic–Jurassic boundary and in the Late Liassic (Giusca et al. 1967; Manzatu et al. 1975; Paraschiv and Soroiu 1984; Pop et al. 1985). K-Ar ages on samples from the metamorphic basement and Hercynian granites (analysed in the Geochronological Laboratory of the Geological Survey of Israel – unpublished data) indicate mostly Late Triassic, Liassic and Early Cretaceous events.

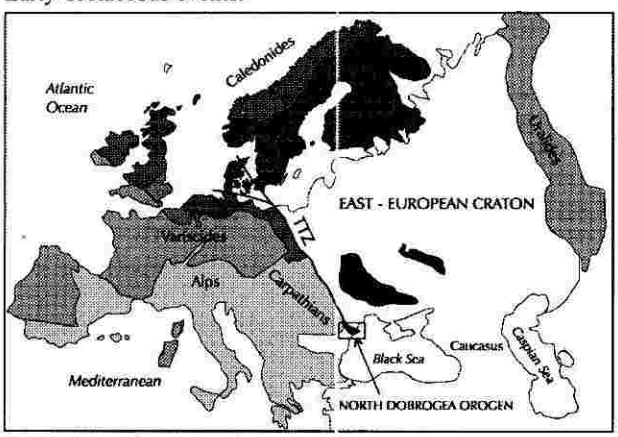

Fig. 1. Location map of North Dobrogea.

This paper includes the first radiometric ages of the basalts from North Dobrogea and represents only a first step in a more reliable study based on the Ar-Ar method.

Geological setting

North Dobrogea is the exposed part of the Cimmerian orogenic belt located north of the Moesian Platform and west of the Black Sea (Fig. 1). It is a narrow belt, 140 km long and 60 km wide, bordered by strike-slip faults. The internal structure of North Dobrogea consists of high-angle thrusts and faults (Baltres 1993; Seghedi et al. 1996). The Hercynian basement is exposed mostly in the western part of the area. Only a few outcrops of basement rocks covered by Triassic to Jurassic sequences are scattered in the east (Fig. 2). In the southern part of North

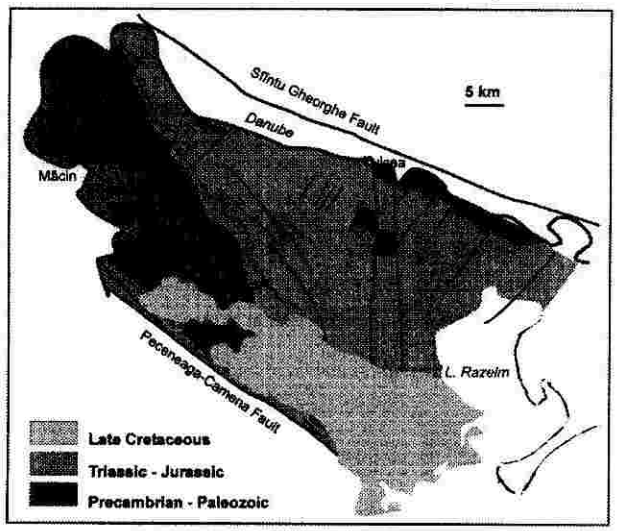

Fig. 2. Simplified subcrop map of North Dobrogea, showing the distribution of the Precambrian–Paleozoic basement, Triassic–Jurassic sediments and the Late Cretaceous post-tectonic cover.

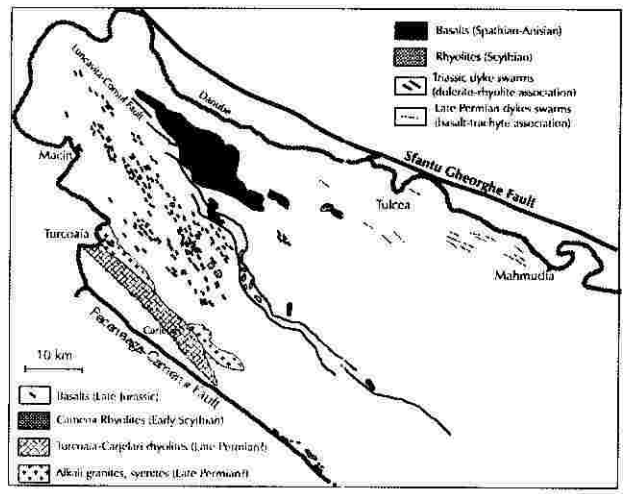

Fig. 3. Distribution of extension-related magmatism in North Dobrogea.

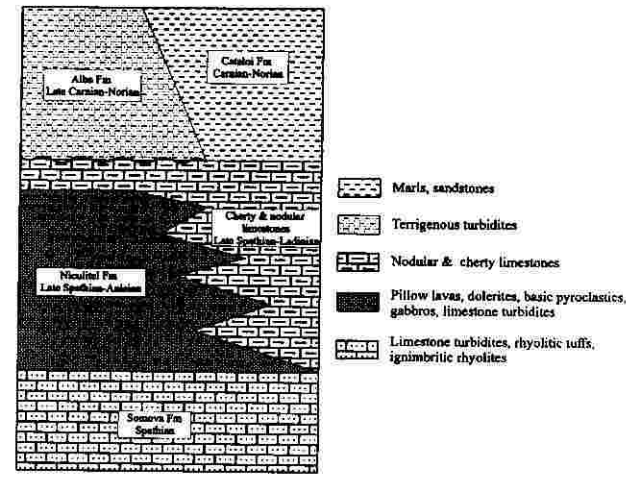

Fig. 4. Simplified chart showing the geological relationships of the Niculitel Formation with other Triassic sediments.

Dobrogea Upper Cretaceous shelf deposits unconformly onlap various basement and older cover rocks.

The Early Alpine evolution started in the Upper Permian, when alkaline rocks intruded the newly consolidated Hercynian basement, thickened by thrusting. During the Lower Scythian (Lower Spathian), as a result of an explosive rhyolitic volcanism, pyroclastic flows and ash fall tuffs were interbedded either with continental red volcaniclastic-epiclastic sequences, or with shallow marine red siliciclastic sequences (Seghedi et al. 1990, 1992; Baltres et al. unpublished data). By the end of the Scythian, the entire rift basin was covered by sea water and carbonate facies sediments accumulated. Basinal Triassic sequences of the Alpine facies occur in the central and northern part of North Dobrogea, while isochronous carbonate platform facies developed to the east (Baltres 1993).

Coeval and following the rhyolitic volcanism, submarine basalts erupted and were deposited in association with limestone turbidites. The emplacement of the pillow basalts was related to basin deepening processes in Late Scythian–Middle Anisian. Probably during the same period of time, NW–SE-trending dyke swarms of basalt–rhyolite bimodal association were emplaced in the Hercynian basement of North Dobrogea (Seghedi 1985; Nicolae and Seghedi 1996) (Fig. 3). They may represent feeding channels of the rhyolitic and basaltic volcanoes, now exposed in the strongly inverted western part of the North Dobrogean rift.

Basalts of the Niculitel Formation

The Niculitel Formation consists mainly of basalts (massive or pillow-lava) and some volcaniclastic pyroclastic rocks and dykes or small gabbroic bodies (Savu et al. 1980; Savu 1986). The basic rocks are interbedded with thin limestone turbidites, basic volcaniclastic turbidites and pelagic limestone (Baltres et al. 1994, unpublished report). The age of the volcanic pile is considered Triassic on the basis of stratigraphic relations: the basalts overlie Spathian limestone turbidites and are overlain by Late Carnian terrigenous turbidites (Fig. 4). Both limestone and terrigenous turbidites are paleontologically dated. The Late Scythian–Anisian age of the basic eruptions is suggested by the conodont assemblages from limestone interbeds in the basaltic sequence (Mirauta 1982).

Field relations indicate at least two events of basalt emplacement (Seghedi et al. 1990). The first is prior or coeval with the beginning of acid volcanic activity. The second event is represented by the dolerite bodies from the Malciu Hill, emplaced after the deposition of both main limestone sequence and the rhyolite flows (Savul 1935; Seghedi et al. 1990).

Basic lava flows show aphanitic or porphyritic texture, with typical intersertal or subophitic structure. The mineralogy is dominated by plagioclase, clinopyroxene (titanaugite), opaque minerals and chloritized glass. The primary minerals are variably replaced by secondary phases: calcite, albite, epidote, chlorite, amphibole. Pumpellyite, prehnite, calcite and chalcedony occur in vesicles, veins or replace primary minerals. The thin beds of basic tuffs and tuffites, interbedded with limestone, consist of albitized plagioclase clasts, pyroxene altered to epidote, chlorite and clay minerals and a variable amount of terrigenous clasts (quartz, quartzite, carbonate). The mafic sills display ophitic or intergranular textures and massive structures, with a better crystallinity than the lava. They consist mainly of plagioclase, clinopyroxene and opaque minerals, partially replaced by secondary phases.

Samples and sample preparation

Three samples of basalts were collected for this preliminary K-Ar survey. The location and mineralogical characteristics of these samples are shown in Table 1.

Field samples of ca. 2 kg each were crushed and sieved (70–90 mesh), and washed with water, alcohol and acetone. Magnetic separation was performed with a Frantz separator. The samples were subsequently leached using 0.5 N HCl for one hour.

Total silicate analyses were performed on the prepared samples for age determination. The main purpose was to better understand the intensity and character of the secondary transformation affecting especially the K-bearing minerals. The analytical results are shown in Table 2.

Analytical method and results

The K concentration of each prepared sample was measured in duplicate by atomic absorption. The error is assumed to be less than 2%. Prior to Ar extraction, samples (wrapped in low Ar blank aluminum foil) were baked for 8–12 hours at ca. –180 °C. Ar extraction was conducted in a molybdenum crucible by melting through induction heating in a metal line. The system attains vacuum in the range of 1×10^{-9} mbar.

Ar isotopes were analysed on a MM-1200 B mass spec-

Sample	Location	Coordinates	Rock Type	Rock Description
RID-4	Piatra Rosie Hill	45°11' 28°50'	Dolerite	Massive, ophitic structure. Plagioclase variably replaced by pumpellyite, prehnite, albite. Fresh Ti-augite. Olvine substituted by chlorite, titanite. Other secondary minerals: amphibole, phylosilicate (?)
RID-5	Piatra Rosie Hill	45°11'10" 28°40'	Dolerite	Ti-augite and plagioclase substituted by prehnite. Chlorite filling vesicules.
RID-6	Asan Hill Revarsarea Quarry	45°15'55" 28°22'50"	Basalt pillow lava	Plagioclase substituted by albite, pumpellyite, prehnite. Augite, magnetite. Calcite-pumpellyite, titanite, albit-pumpellyite and calcite-epidote veinlets

Tab. 1. Sample description.

trometer. The sensitivity of the mass spectrometer, equipped with a Faraday cup, is 2.6×10^{-4} Amp/Torr. Extraction line blanks show constant values (5×10^{-9} cc STP of ^{40}Ar) which generally has an atmospheric $^{40}Ar/^{36}Ar$. A typical sample has about 1×10^{-6} cc STP of ^{40}Ar (4.46×10^{-11} moles). The mean value of the ratio $^{40}Ar/^{36}Ar$ of atmospheric Ar is routinely measured with a precision exceeding 0.5% of the ratio. Calibration of the ^{38}Ar spike is performed using LP-6 standard biotite and the uncertainty is ± 0.5%. The constants used are according to IUGS (Steiger and Jäger 1977).

Uncertainties on a single measurement were calculated using the Gauss method as described by Heimann (1990). Mean uncertainties from multiple samples at a single site were derived using a formulation taking into account the uncertainty of each individual determination and the dispersion of ages of multiple samples of each site. This approach results in a larger uncertainty than would be implied by single standard deviation on all the ages, and probably represents the actual uncertainties better than less conservative estimates (for more details see Heimann 1990 and Heimann and Ron 1993).

The K-Ar results are shown in Table 3. Each sample was measured two or three times and the age is a calculated mean value. Samples RID-4, RID-5 (whole rock) and RID-6 (low magnetic fraction) yielded similar values within the analytical error. The age of the high magnetic separate of RID-6 is older (141.9 ± 2.1) and was yielded by very similar duplicate measurements.

Discussion

The K-Ar results plotted in a $^{40}Ar/^{36}Ar$ versus $^{40}K/^{36}Ar$ diagram (Fig. 5) yielded a good isochron with a calculated age of 132.7 ± 1.5 Ma. (Late Valanginian). It is considered (e.g. Faure 1986) that only cogenetic minerals and/or whole rocks with similar geologic history form isochrons. The calculated initial $^{40}Ar/^{36}Ar$ ratio (297.7) is very close to the atmospheric ratio (295.5). This is usually considered an indication that the rocks and/or minerals plotted in the isochron remained closed to both Ar and K since their cooling. A conclusion based on the K-Ar isochron age would suggest that the Early Cretaceous age is the primary cooling age of the studied basalts. Nevertheless, the stratigraphic position of the basaltic rocks is, as already mentioned, Triassic. The secondary alterations affecting the K-bearing minerals may lead to a certain degree of resetting of the K-Ar clock. On the other hand, the secondary transformation is not evident in the chemical analyses characterized by a relative low loss on ignition (Table 2).

At this stage of the study, the most plausible interpretation is to consider the Alpine deformations as the cause of the resetting of the K-Ar system. Obviously, further and more detailed geochronological work (e.g. Ar-Ar dating on monomineral fractions) is necessary in order to understand the real significance of the radiometric ages of the Niculitel basalts.

Acknowledgments

The study was partly supported by a grant from the Romanian Ministry of Research and Technology. The K-Ar and total silicate analyses were performed at and supported by the Geological Survey of Israel. Thanks are due to C. Dallal for his contribution at the geochronological laboratory, to D. Stiber for potassium determination and to S. Erlich for the chemical analyses.

	RID-4	RID-5	RID-6 (LM)	RID-6 (HM)
SiO_2	45.5	48.5	49.5	46.9
Al_2O_3	8.3	16.1	15.6	15.9
Fe_2O_3	11.3	9.3	9.8	11.6
TiO_2	3.7	1.9	2.1	1.8
CaO	14.2	7.8	9.1	9.0
MgO	11.9	7.0	6.2	6.7
MnO	0.18	0.12	0.15	0.13
P_2O_5	< 0.1	< 0.1	< 0.1	< 0.1
SO_3	< 0.1	< 0.1	< 0.1	< 0.1
K_2O	0.7	1.1	1.4	0.9
Na_2O	1.1	3.7	3.0	3.0
LOI	2.3	3.8	2.7	3.2
Total	99.2	99.3	99.6	99.1

Tab. 2. Chemical analyses of the K-Ar samples. LM – Low magnetic separation; HM – High magnetic separation.

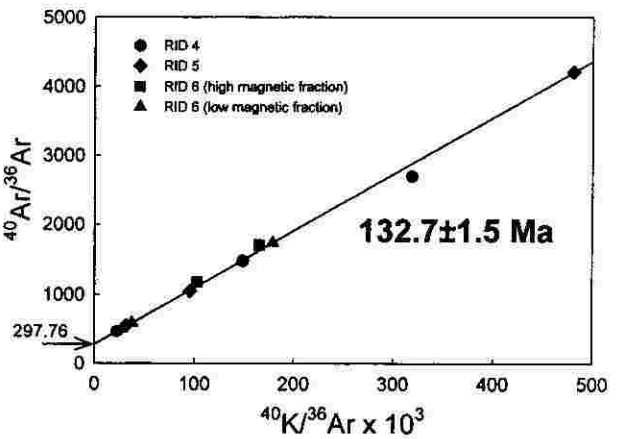

Fig. 5. K-Ar isochron of the Niculitel basalt samples.

Sample No.	Magnetic Separation	K (%)	^{40}Ar Rad. (%)	^{40}Ar Rad CC STP/gr X10^{7}	Age (Ma)	Error (Ma)	Mean Age (Ma)
4	WR	0.62	89.04	3.110	125.22	2.52	
4	WR	0.62	36.41	3.082	124.12	2.71	127.3 ±4.8
4	WR	0.62	80.10	3.297	132.50	2.66	
5	WR	0.97	92.98	5.261	134.81	2.71	
5	WR	0.97	46.34	5.140	131.81	2.89	132.5 ±2.6
5	WR	0.97	71.91	5.105	130.96	2.62	
6	HM	1.14	74.98	6.572	142.42	2.84	141.9 ±2.1
6	HM	1.14	82.70	6.526	141.46	2.84	
6	LM	0.81	83.02	4.355	134.06	2.69	
6	LM	0.81	40.27	3.971	122.66	2.54	128.2 ±5.9
6	LM	0.81	49.56	4.148	127.92	2.78	

Tab. 3. K-Ar analytical data. WR – Whole rock; HM – High magnetic fraction; LM – Low magnetic fraction.

References

BALTRES A. 1993. *Somova Formation (North Dobrogea) Sedimentological study*. MS, Ph.D. Thesis, Bucharest University. Bucuresti.

FAURE G. 1986. *Principles of isotope geology*. J. Wiley and Sons, 560 pp. New York.

GIUSCA D., IANOVICI V., MANZATU S., SOROIU M., LEMNE M., TANASESCU A. and IONCICA M. 1967. Asupra varstei absolute a formatiunilor cristalofiliene din forlandul orogenului carpatic. *St. Cerc. Geol. Geofiz. Geogr., ser. Geol.*, 12, 287–297.

HEIMANN A. 1990. *The development of the Dead Sea Rift and its margins in northern Israel during the Pliocene and the Pleistocene*. Ph.D. Thesis. Hebrew Univ., Jerusalem, 114 pp (in Hebrew, English abstract).

HEIMANN A. and RON H. 1993. Geometrical changes of plate boundaries along part of the northern Dead Sea transform: geochronologic and paleomagnetic evidence. *Tectonics*. 12, 477–491.

MIRAUTA E. 1982. Biostratigraphy of the Triassic deposits in the Somova–Sarica Hill zone (North Dobrogea) with special regard of the eruption age. *D. S. Inst. Geol. Geof.*, 64/4, 63–78.

MANZATU S., LEMNE M., VAJDEA E., TANASESCU A., IONCICA M. and TIEPAC, I. 1975. Date geocronologice absolute pentru formatiuni cristalofiliene si masive eruptive in Romania. *D. S. Inst. Geol. Geofiz.*, 61 (5), 85–111.

NICOLAE I. and SEGHEDI A. 1996. Lower Triassic basic dyke swarms in North Dobrogea. *Rom. J. Petrol.*, 77, 31–40.

PARASCHIV D. and SOROIU M. 1984. Date geocronologice asupra unor roci metamorfice si eruptive din Promontoriul nord-dobrogean. *Mine, Petrol si Gaze*, 35 (9), 456–458.

POP G., BUZILA A., CIOLOBOC D., CATILINA D. and POPESCU G. 1985. Isotopic Rb-Sr ages for establishing the emplacement sequence of some granitoids of North Dobrogea. *Proc. Rep. of the XIII CBGA*, Krakow, 108–111.

RADAN S. 1994. Relicts of paleoweathering crusts in Dobrogea. *Analele Univ. Buc., Geologie*, abstr. vol. suppl., AN 43, 28.

SAVU H., UDRESCU C. and NEACSU V. 1980. Structural, petrological and genetic study of the ophiolites from the Niculitel zone (North Dobrogea). *D. S. Inst. Geol.* 65 (1), 41–64.

SAVU H. 1986. Triassic, continental intra-plate volcanism in North Dobrogea. *Rev. Roum. Geol. Geoph. Geogr., Geologie*, 30, 21–29.

SAVUL M. 1935. Porphyres quartziferes de la region Meidanchioi–Consul (Dobrogea du Nord). *C. R. Inst. Geol. Rom.* 20, 86–99.

SEGHEDI A. 1985. Variszische Faltung in alpidischen Einheiten der Nord Dobrudscha. *Z. angew. Geol.*, 31, 11.

SEGHEDI A., AVRAM E. and POPESCU G. 1996. Dobrogea. In *Conferinta IGR-90, Bucuresti 1996, Excursion Guide A, South Carpathians–Apuseni Mountains–East Carpathians–Dobrogea. An. Inst. Geol.*, 69, supl. 2, 51–71.

SEGHEDI, I., SZAKACS A. and BALTRES A. 1990. Relationships between sedimentary deposits and eruptive rocks in the Consul unit (North Dobrogea). Implications on tectonic interpretations. *D. S. Inst. Geol.Geofiz.*, 74 (5), 125–136.

SEGHEDI I., SZAKACS A., UDRESCU C., GRABARI G., STOIAN M., TANASESCU A. and VLAD C. 1992. Major and trace element geochemistry of rhyolites from northern Dobrogea. Petrogenetic implications. *Rom. J. Petrol.*, 75, 17–38.

STEIGER R.H. and JÄGER E. 1977. Subcommission on Geochronology: Convention on the use of decay constants in geo- and cosmochronology. *Earth Planet. Sci. Lett.*, 36, 359–362.